Finite-difference solution of the image wave equation for depth remigration

J. Schleicher, A. Novais and F. P. Munerato, IMECC-UNICAMP, Campinas (SP), Brazil

This paper was prepared for presentation at the 8th International Congress of The Brazilian Geophysical Society held in Rio de Janeiro, Brazil, 14-18 September 2003.

Abstract

The image wave equation for depth remigration is a partial differential equation that is similar to the acoustic wave equation. In this work, we determine the stability conditions that have to be met when solving the image wave equation by finite differences. The stability criterion exhibits a strong wavenumber dependence. Where higher horizontal than vertical wavenumbers are present in the data to be remigrated, stability may be difficult to achieve. Numerical tests demonstrate that the implementational form of the chosen FD scheme can be essential to obtain results with a limited numerical error even in situations where stability cannot be theoretically guaranteed.

Introduction

Seismic remigration is an imaging technique that envisages the construction of an improved migrated section for an updated macrovelocity model on the basis of a previously migrated section as obtained with a different initial macrovelocity model. If the two macrovelocity models do not differ too much, one generally calls the imaging procedure that corrects the image a "residual migration" (Rothman et al., 1985). Where significant differences between both models are allowed, the process is referred to as remigration (Hubral et al., 1996) or velocity continuation (Fomel, 1994).

The sequence of images of a certain reflector as subsequently migrated with varying migration velocities creates an impression of a propagating wavefront. This "propagating wavefront" was termed an "image wave" by Hubral et al. (1996). The propagation variable, however, is not time as is the case for conventional physical waves as described, e.g., by the acoustic wave equation, but the migration velocity.

For homogeneous media, Hubral et al. (1996) have studied the kinematic behaviour of these image waves as a function of the constant migration velocity. By treating them like conventional acoustic waves, they derived partial differential equations, termed "image wave equations," that describe the "propagation" of the reflector image as a function of migration velocity for both, time and depth remigration.

The image wave equation for time remigration has already been theoretically studied and implemented, successfully applied to real data from ground-penetrating radar (Jaya et al., 1999, see also references there). In this work, we derive the image wave equation for depth remigration in 3-D, choose an FD scheme for its implementation, as well as theoretically and numerically study its consistency and stability.

The 3-D image wave equation for depth remigration

We consider a zero-offset experiment with coincident sources and receivers at positions described by coordinates ξ and η on the planar earth surface. Let Σ_0 be a reflector image that was obtained by a migration of zero-offset data using an incorrect migration velocity, v_0. The aim is to construct from Σ_0 the reflector image Σ that would have been obtained if the data had been migrated with the correct velocity v.

The input reflector image Σ_0 is considered as a set of points P_0. Each of these points $P_0 = (x_0, y_0, z_0)$ in the input velocity model is kinematically equivalent to a surface $z = \mathcal{Z}(x, y)$ in the output velocity model, i.e., both generate the same zero-offset reflection-time surface $t(\xi, \eta)$, i.e.,

$$\begin{aligned} t(\xi,\eta) &= \frac{2}{v}\sqrt{(\xi-x)^2+(\eta-y)^2+z^2} \\ &= \frac{2}{v_0}\sqrt{(\xi-x_0)^2+(\eta-y_0)^2+z_0^2}\,. \end{aligned} \qquad (1)$$

The envelope of these equivalent surfaces provides the new reflector image, in the same way as a physical wavefront is the envelope of Huygens waves originating at secondary sources along the previous wavefront. Therefore, these equivalent surfaces are referred to as "Huygens image waves" (Hubral et al., 1996).

A Huygens image wave can be constructed as the envelope of the isochrons of all points on the traveltime surface $t(\xi, \eta)$. Taking the derivatives of identity (1) with respect to ξ and η, equaling them to zero and substituting the results back into equation (1) yields the following formula for the 3-D Huygens image wave,

$$z = \mathcal{Z}(x,y) = v\sqrt{\frac{1}{v_0^2}z_0^2 + \frac{1}{v_0^2-v^2}\left[(x-x_0)^2+(y-y_0)^2\right]}\,. \qquad (2)$$

Solution of equation (2) for v yields an equation of the form $v = \mathcal{V}(x, y, z)$, where $\mathcal{V}$ is the eikonal of the image wave. We now substitute $v = \mathcal{V}(x, y, z)$ in equation (2) and differentiate implicitely with respect to x, y, and z. Then, we use the three resulting expressions to eliminate $x - x_0$, $y - y_0$,

and z_0 from equation (2). Denoting the partial derivatives of $\mathcal{V}$ by $\mathcal{V}_x$, $\mathcal{V}_y$, and $\mathcal{V}_z$, respectively, the result reads

$$\mathcal{V}_x^2 + \mathcal{V}_y^2 + \mathcal{V}_z^2 - \frac{\mathcal{V}}{z}\mathcal{V}_z = 0\ . \tag{3}$$

This is the 3-D image eikonal equation. The last step is to find a second-order differential equation for the "image wavefield" $p(x,y,z)$ such that a substitution of the ray ansatz $p(x,y,z) = p_0(x,y,z)f(v - \mathcal{V}(x,y,z))$ yields the above eikonal equation. Here, p_0 is the amplitude of the migrated reflector image, i.e., the image wave, and $f(v)$ is the source wavelet as a function of velocity. The simplest differential equation that fulfills the above requirement is

$$p_{xx} + p_{yy} + p_{zz} + \frac{v}{z}p_{vz} = 0\ . \tag{4}$$

To arrive at the eikonal equation (3) upon substitution of the above ray ansatz in equation (4), one needs to substitute v by $\mathcal{V}(x,y,z)$. This substitution is valid on the image wavefront $v = \mathcal{V}$ itself. However, points off the wavefront are also involved in the propagation of the image. As we will see in the numerical example, this leads to a stretch of the wavelet in the propagating image.

Finite differences

We consider a grid of depth points with initial point at (x_i, y_i, z_i) and a discretized velocity axis. The image wavefield at a given grid point $(x_k, y_l, z_m) = (x_i + k\Delta x, y_i + l\Delta y, z_i + m\Delta z)$, as calculated for a certain migration velocity $v_n = v_0 + n\Delta v$, is denoted by $p^n_{k,l,m}$. On this grid, we approximate the derivatives in equation (4) by finite differences. For the spatial derivatives, we use fourth-order approximations, and for the mixed derivative, we choose a first-order scheme forward in v and z. Using these approximations for the derivatives in the image wave equation (4) and isolating $p^{n+1}_{k,l,m+1}$, we find the following FD scheme,

$$\begin{aligned} p^{n+1}_{k,l,m+1} &= -\frac{z_m \Delta v \Delta z}{12 v_n}\left\{\delta^{(2)}_{x,4}p + \delta^{(2)}_{y,4}p + \delta^{(2)}_{z,4}p\right\} \\ &\quad + p^{n+1}_{k,l,m} + p^{n}_{k,l,m+1} - p^{n}_{k,l,m}\ , \end{aligned} \tag{5}$$

where $\delta^{(2)}_{x,4}p$, $\delta^{(2)}_{y,4}p$, and $\delta^{(2)}_{z,4}p$ denote the spatial fourth-order finite-difference approximations of the spatial second derivatives p_{xx}, p_{yy}, and p_{zz}, respectively. The initial condition is given by the original migrated section for the velocity v_0. As boundary conditions, we use that the field outside the given target zone of the input section should be zero.

Since the FD scheme (5) is an implicit one, its computation would require the solution of a linear system of equations in each step. Such a procedure would, of course, be expensive to realize, particularly for large migrated sections. For this reason, we prefer to treat equation (5) as an explicit scheme. This requires an additional boundary condition to initialize the loop in z. We choose again a homogeneous boundary condition.

Consistency, stability, and grid dispersion.

In order to actually use the FD scheme (5), its consistency and stability need to be investigated, so as to find conditions for the step size Δv as a function of the medium parameters and the grid intervals Δx, Δy, and Δz. As can be readily verified, scheme (5) is indeed consistent with the differential equation (4). To determine the conditions under which this scheme is stable, we apply the von Neumann criterion (see, e.g., Thomas, 1995). It consists of substituting the Fourier component

$$p^n_{k,l,m} = \xi^n \exp\{ik\kappa_x\Delta x\}\exp\{il\kappa_y\Delta y\}\exp\{im\kappa_z\Delta z\} \tag{6}$$

in scheme (5), where ξ is the so-called amplification factor. An FD scheme is known to be stable, if $|\xi| < 1$. The grid dispersion is described by the phase of ξ Strikwerda (1989).

From substitution of the discrete Fourier transform (6) in equation (5) and solution of the resulting equation for ξ, we find the expression

$$\xi = \frac{4\Lambda}{(e^{i\kappa_z\Delta z} - 1)} + 1, \tag{7}$$

where

$$\begin{aligned} \Lambda &= \frac{z_m}{3v_n}\frac{\Delta v \Delta z}{(\Delta x)^2}\sin^2\frac{\kappa_x\Delta x}{2}\left[3 + \sin^2\frac{\kappa_x\Delta x}{2}\right] \\ &\quad + \frac{z_m}{3v_n}\frac{\Delta v \Delta z}{(\Delta y)^2}\sin^2\frac{\kappa_y\Delta y}{2}\left[3 + \sin^2\frac{\kappa_x\Delta y}{2}\right] \\ &\quad + \frac{z_m}{3v_n}\frac{\Delta v \Delta z}{(\Delta z)^2}\sin^2\frac{\kappa_z\Delta z}{2}\left[3 + \sin^2\frac{\kappa_z\Delta z}{2}\right]. \end{aligned} \tag{8}$$

Thus, the von Neumann condition $|\xi| \le 1$ provides the stability condition

$$0 \le \Lambda \le \sin^2\frac{\kappa_z\Delta z}{2}. \tag{9}$$

Note that equation (9) must be satisfied for all wavenumbers κ_x, κ_y, and κ_z involved in the remigration problem to be solved. This can be a difficult condition to meet. The simplest situation is the case where wavenumbers and grid increments are of the same size, such that $\Delta x = \Delta y = \Delta z$ and $\kappa_x\Delta x \approx \kappa_y\Delta y \approx \kappa_z\Delta z$. In this situation, the above condition can be divided by $\sin^2\frac{\kappa_z\Delta z}{2}$ to yield

$$\begin{aligned} 0 < \frac{4z_{\max}}{3v_{\min}}\frac{\Delta v}{\Delta z} + \frac{4z_{\max}}{3v_{\min}}\frac{\Delta v}{\Delta z} + \frac{4z_{\max}}{3v_{\min}}\frac{\Delta v}{\Delta z} \le 1 \\ \Longrightarrow \quad \Delta v \le \frac{1}{4}\frac{v_{\min}}{z_{\max}}\Delta z, \end{aligned} \tag{10}$$

where we have used that $3 + \sin^2\frac{\kappa_z\Delta z}{2} \le 4$. Moreover, we have replaced z_m and v_n by their maximum and minimum values, $z_{\max}$ and $v_{\min}$, respectively. The right-hand-side expression of the last inequality in equation (10) can be multiplied by 3 if the horizontal wavenumbers are very small, i.e., $\kappa_x \approx \kappa_y << \kappa_z$.

The term $\sin^2\frac{\kappa_z\Delta z}{2}$ on the right-hand side of equation (9) has an important consequence for the stability of the FD

scheme (5). If there are vertical wavenumbers κ_z present in the data for which this term is very close to zero, it will be very hard very small values of Δv might be needed to make the scheme stable.

For the grid dispersion, we have to analyze the phase of the von Neumann amplification factor ξ. In a Taylor series up to second order in Δv and the spatial grid sizes Δx, Δy, and Δz, we find

$$\arg \xi = k\alpha\Delta v \approx \frac{k^2 z_m}{\kappa_z v_n}\Delta v + \frac{k^4 z_m^2}{2\kappa_z v_n^2}\Delta v^2 \Delta z - \frac{k_z k^2 z_m}{12 v_n}\Delta z^2 \Delta v \ , \tag{11}$$

where $k^2 = \kappa_x^2 + \kappa_y^2 + \kappa_z^2$ and α is the image-wave propagation velocity. Note that α depends on z_m, i.e., the propagation velocity is different at different depths. Moreover, we observe that the image wave equation possesses intrinsic dispersion since the main term of α depends on the spatial frequencies as k/k_z. Grid dispersion can be reduced to a minimum if we can choose Δz and Δv such that the second an third terms in expression (11) cancel each other. This implies

$$\Delta v = \frac{1}{6}\frac{\kappa_z^2}{k^2}\frac{v_n}{z_m}\Delta z \approx \begin{cases} \frac{1}{18}\frac{v_n}{z_m}\Delta z & \text{if } \kappa_x \approx \kappa_y \approx \kappa_z \\ \frac{1}{6}\frac{v_n}{z_m}\Delta z & \text{if } \kappa_x \approx \kappa_y << \kappa_z \end{cases} . \tag{12}$$

This expression means that grid dispersion is depth dependent. Thus, it cannot be fully eliminated from the propagating image as long as we wish to work with a constant grid size. Still, we can try to approximately satisfy equation (12) at least for the estimated values of the velocity and the depth of the target reflector.

Numerical tests

To demonstrated the FD image-wave remigration, we had to restrict scheme (5) to the corresponding 2-D one, in order to meet the computational limitations. We have used migrated data from a simple earth model consisting of two homogeneous halfspaces, separated by a horizontal reflector at a depth of 550 m. The velocities above and below the reflector are $c_1 = 3$ km/s and $c_2 = 3.5$ km/s. The simulated seismic survey is a zero-offset experiment with 401 source-receiver pairs, located at every 10 m between -2000 m and 2000 m along the x-axis.

The input data to the remigration where generated by a zero-offset depth migration with a wrong migration velocity of $v_0 = 2$ km/s. The resulting depth image is depicted in Figure 1a. Note that the wrong migration velocity causes the reflector to be imaged at a wrong depth of about 370 m.

This input section was then remigrated using FD scheme (5). The grid size of the depth region was $\Delta x = \Delta z = 10$ m and $\Delta v = 4$ m/s. This is in accordance with the 2-D version of stability condition (10) (where the factor $1/4$ is replaced by $3/8$). Parts b and c of Figure 1 show two snapshots of the image wave for velocities $v = 2.4$ km/s and $v = 3$ km/s, the latter being the true medium velocity. We observe that the reflector image in Figure 1c is remigrated to the correct

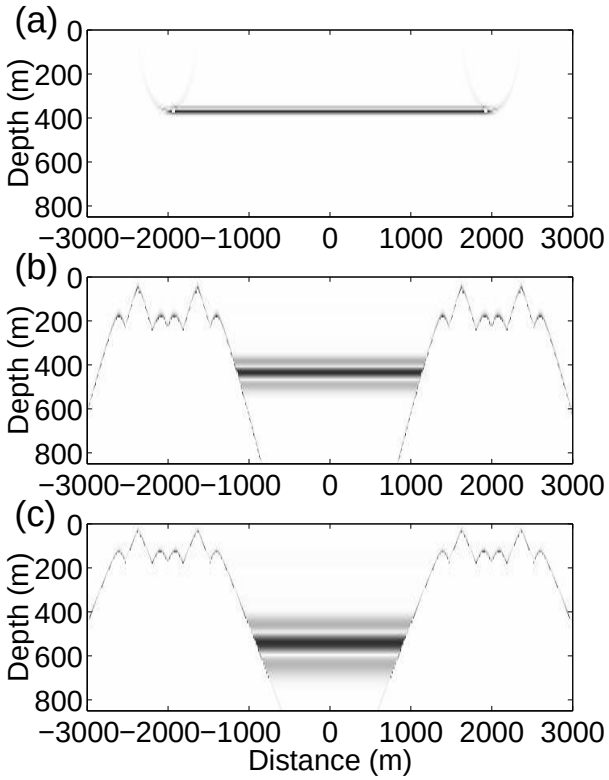

Figure 1: Image wave propagation. Direct implementation. (a) Input data for the remigration example: data after migration with a wrong migration velocity of $v_0 = 2$ km/s. (b) Remigrated image for $v = 2.4$ km/s. (c) Remigrated image for $v = 3$ km/s.

depth of 550 m. There are, however, quite large regions where the image is obscured by noise, which is many orders of magnitude larger than the actual image. In fact, in Figure 1, the error was zeroed out wherever it exceeds the amplitude of the reflector image.

The reason for this noise to arise, although stability condition (10) is satisfied, is a violation of the stricter condition (9) at the tips of the migration boundary effects (smiles). Here, the image contains much higher wavenumbers in the horizontal than in the vertical direction. As a consequence, the right-hand side of equation (9) becomes smaller than the left-hand side. This causes an instability that gives rise to the error.

There is, however, a way to obtain a better remigration result with scheme (5). Figure 2 depicts the results of an FD remigration using scheme (5) in reverse implementation. In other words, the results in Figure 2 where obtained by solving equation (5) for $p_{k,l,m}^{n+1}$.

The reason for the different results of Figures 1 and 2, although obtained from implementations of the same FD scheme and thus governed by the same stability conditions, is the multiplication by z_m in scheme (5). In the direct implementation, numerical errors generated at one

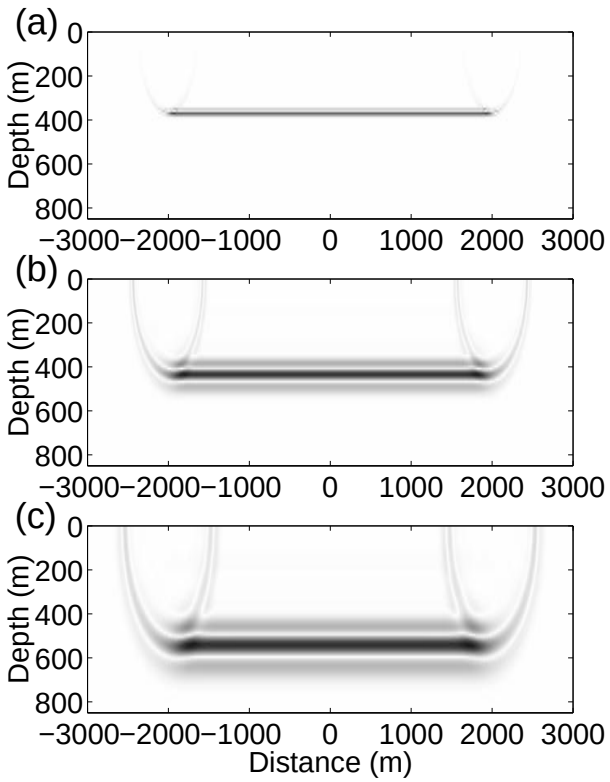

Figure 2: Image wave propagation. Reverse implementation. (a) Input data for the remigration example: data after migration with a wrong migration velocity of $v_0 = 2$ km/s. (b) Remigrated image for $v = 2.4$ km/s. (c) Remigrated image for $v = 3$ km/s.

step are multiplied by increasing values of z_m in subsequent steps, leading to an exponentially increasing error. In the reverse implementation, decreasing values of z_m lead to a damping of the error.

As a final observation, let us comment on the pulse stretch of FD remigration (Figures 1 and 2). It is much stronger than the conventional pulse stretch due to depth migration, which is proportional to the migration velocity (Tygel et al., 1994). The reason that causes the additional stretch is the substitution of $\mathcal{V}$ by v in the derivation of the image wave equation (4). This means that off the reflector, a slight error is introduced into the kinematic behavior of the pulse. In effect, this causes the upper part of the pulse to be moved to shallower depths than it should be, while at the same time the lower part of the pulse is moved to greater depths.

Conclusions

The image wave equation for depth remigration is a second-order partial differential equation that describes the "propagation" of a migrated reflector image as a function of a changing migration velocity (Hubral et al., 1996). In this work, we have studied the consistency and stability of an FD scheme for this equation. The theoretical stability condition obtained from the von Neumann criterion points towards general difficulties of the process when remigrating data containing large wavenumbers in the horizontal directions. Numerical tests have demonstrated that instabilities indeed arise in such situations. They can, however, be controlled by using an implementation of the FD scheme in the reverse vertical direction.

With the investigated FD schemes, reflector images can be remigrated only either to larger or to smaller migration velocities. The scheme forward in v and forward in z allows only for an increase, the scheme forward in v and backward in z only for a decrease of the migration velocity. Other FD schemes that may be less restrictive are currently under investigation.

We have seen that image-wave propagation suffers from intrinsic dispersion as well as grid dispersion due to chosen FD scheme. Since the grid dispersion depends on velocity and depths as well as on the spatial frequencies, it cannot be entirely eliminated. It can, however, be reduced by an appropriate choice of the grid size.

A drawback of image-wave remigration is its exaggerated pulse strech. It degrades the vertical resolution of the remigrated image. The effect is inherent to the method as it is introduced by the very image wave equation that describes the propagation of the reflector image.

Acknowledgements

This work was kindly supported by the CNPq and FAPESP, Brazil, and the sponsors of the *Wave Inversion Technology (WIT) Consortium*, Karlsruhe, Germany.

References

Fomel, S., 1994, Method of velocity continuation in the problem of seismic time migration: Russian Geology and Geophysics, **35**, no. 5, 100–111.

Hubral, P., Tygel, M., and Schleicher, J., 1996, Seismic image waves: Geophys. J. Internat., **125**, no. 2, 431–442.

Jaya, M., Botelho, M., Hubral, P., and Liebhardt, G., 1999, Remigration of ground-penetrating radar data: J. Appl. Geoph., **41**, 19–30.

Rothman, D., Levin, S., and Rocca, F., 1985, Residual migration: Applications and limitations: Geophysics, **50**, no. 1, 110–126.

Strikwerda, J., 1989, Finite difference schemes and partial differential equations: Wadsworth & Brooks, California.

Thomas, J., 1995, Numerical partial differential equations: Springer-Verlag, New York.

Tygel, M., Schleicher, J., and Hubral, P., 1994, Pulse distortion in depth migration: Geophysics, **59**, no. 10, 1561–1569.